

AHR Regulates WT1 Genetic Programming during Murine Nephrogenesis

M Hadi Falahatpisheh, Adrian Nanez, and Kenneth S Ramos

Department of Biochemistry and Molecular Biology, University of Louisville School of Medicine, Louisville, Kentucky, United States of America

Mounting evidence suggests that the blueprint of chronic renal disease is established during early development by environmental cues that dictate alterations in differentiation programming. Here we show that aryl hydrocarbon receptor (AHR), a ligand-activated basic helix-loop-helix-PAS homology domain transcription factor, disrupts murine renal differentiation by interfering with Wilms tumor suppressor gene (WT1) signaling in the developing kidney. Embryonic kidneys of C57BL/6J *Ahr*^{-/-} mice at gestation d (GD) 14 showed reduced condensation in the nephrogenic zone and decreased numbers of differentiated structures compared with wild-type mice. These deficits correlated with increased expression of the (+) 17aa *Wt1* splice variant, decreased mRNA levels of *Igf-1 rec.*, *Wnt-4* and *E-cadherin*, and reduced levels of 52 kDa WT1 protein. AHR knockdown in wild-type embryonic kidney cells mimicked these alterations with notable increases in (+) 17aa *Wt1* mRNA, reduced levels of 52 kDa WT1 protein, and increased (+) 17aa 40-kDa protein. AHR downregulation also reduced *Igf-1 rec.*, *Wnt-4*, *secreted frizzled receptor binding protein-1 (sfrbp-1)* and *E-cadherin* mRNAs. In the case of *Igf-1 rec.* and *Wnt-4*, genetic disruption was fully reversed upon restoration of cellular *Wt1* protein levels, confirming that functional interactions between AHR and *Wt1* represent a likely molecular target for renal developmental interference.

© 2011 The Feinstein Institute for Medical Research, www.feinsteininstitute.org

Online address: <http://www.molmed.org>

doi: 10.2119/molmed.2011.00125

INTRODUCTION

The fetal basis of adult renal disease in humans first was suggested by Barker and colleagues in studies showing that intrauterine growth restriction has a negative influence on the development of the cardiovascular system, and favors the occurrence of hypertension, insulin resistance, hypercholesterolemia and hyperuricemia later in life (1). These findings have been confirmed in experimental animal models of human disease (2,3), indicating that highly conserved signaling pathways exist that control differentiation programming through interaction with environmental cues that define complex genetic interactions at the cellular level. The basic helix-loop-helix (bHLH)-PAS superfamily is a highly conserved group of proteins involved in

mammalian development and the adaptive response to environmental stress (4). AHR (aryl hydrocarbon receptor) is the only member of the superfamily that is conditionally regulated by ligand binding to the PAS domain. In cultured metanephric kidneys, sustained activation of AHR by exogenous ligands is followed by proteasomal degradation of the receptor and inhibition of epithelialization and nephrogenesis (5). An essential role of AHR in spatiotemporal regulation of metanephric development is suggested by the notable deficits in mesenchymal-to-epithelial transition (MET) seen in cultured metanephric kidneys isolated from *Ahr*^{-/-} mice. The developmental functions of *Ahr* may be mediated by physiological ligands generated by aspartate aminotransferase, an en-

zyme that is highly enriched in kidney (6).

WT1 has long been recognized as a critical regulator of nephrogenesis (7). *Wt1* encodes a 52 kDa zinc finger transcription factor involved in renal and gonad development, with exons 1–6 encoding domains involved in transcriptional regulation, dimerization and RNA recognition and exons 7–10 encoding the four zinc fingers within the DNA-binding domain. Multiple protein isoforms are synthesized due to: (a) alternative splicing regions corresponding to the whole of exon 5 (17 amino acids) and to the three last codons of exon 9 (KTS); (b) a site of RNA editing at codon 281 in exon 6 where a C to T transition produces a leucine to proline substitution; (c) a non-AUG initiation codon resulting in *Wt1* proteins with a higher molecular weight; and (d) an internal AUG resulting in *Wt1* proteins with a lower molecular weight of approximately 40 kDa (8). In the kidney, WT1 mRNA species exhibit combinatorial patterns that primarily include variants resulting from exon 5 splicing (+17 and -17 amino acids),

Address correspondence and reprint requests to Kenneth S Ramos, University of Louisville School of Medicine, Louisville, KY 40292. Phone: 502-852-7340; Fax: 502-852-3659; E-mail: kenneth.ramos@louisville.edu.

Submitted April 24, 2011; Accepted for publication August 17, 2011; Epub (www.molmed.org) ahead of print August 18, 2011.

or +KTS and -KTS alternative splice variants from splicing of exon 9. Biochemical and genetic evidence indicates that different *Wt1* isoforms support different cellular functions, with \pm KTS-regulating *Wt1* DNA binding specificity (8). Changes in exon 5 splice variants also are associated with deficits in renal differentiation (9). Addition of 17 amino acids in exon 5 creates an mRNA isoform that regulates transactivation (10). N-terminal residues 1–182 encode a dimerization region implicated in the regulatory mechanism exerted by dominant negative mutants (11). The (-) KTS behaves as a transcription factor that regulates genes expressed during kidney development *in vitro*, including *Igf-2*, *Pdgfra*, *Egfr*, *Pax-2* and *Wt1* itself, while the (+) KTS isoform regulates the splicing machinery of mammalian cells (12). Hammes (13) generated mouse strains that specifically lack the (-) KTS or (+) KTS *Wt1* splice variants and showed that the (+) KTS isoform is important for maintenance of podocyte function. In fact, mice lacking the (+) KTS *Wt1* variant are characterized by development of renal insufficiency with focal and segmental glomerular sclerosis and male-to-female sex reversal, similar to the human Frasier syndrome (14). Only preliminary results have been obtained regarding functional consequences of the presence or absence of the 17 amino acids encoded by exon 5 and containing a protein:protein interaction (15). At the cellular level, the balance between (\pm) exon 5 isoforms may be involved in regulation of proliferation, differentiation and apoptosis and prevention of tumor formation (16).

A functional link between AHR and WT1 was suggested by the previous finding that activation of AHR by benzo(a)pyrene, a hydrocarbon ligand of the receptor, induces the (-) KTS *Wt1* isoform in cultured metanephric kidneys of *Ahr*^{+/+} but not *Ahr*^{-/-} mice (5). Evidence is presented that AHR functions as a regulator of renal cell differentiation through mechanisms that involve changes in the relative abundance of WT1 splice variants and deregulation of downstream WT-1 signaling.

MATERIALS AND METHODS

Animals/Metanephros Harvest

C57bL/6J wild type or *Ahr* knockout mice were purchased from Jackson Laboratory (Bar Harbor, MN, USA) and placed under standard housing conditions. The care, breeding and handling of animals were conducted in accord with NIH guidelines. At d 14 of gestation, mouse embryos were resected from C57bL/6J wild-type or *Ahr* knockout pregnant dams; the developing kidneys were harvested and processed for further analysis *in vivo* as described before (5).

Morphometric Analysis

Embryonic kidneys were fixed by 4% paraformaldehyde. Hematoxylin and eosin (H&E) slides (5- μ m sections) were examined by bright-field light microscopy. Computer-assisted analysis was performed on six to eight histological sections from embryonic developing kidneys of wild-type or *Ahr*^{-/-} mice, respectively. Measurements were taken from serial sections of embryonic kidneys from three or more dams. The values shown represent the composite of serial sections with variance expressed as the difference between values for each kidney per mouse strain. Images were captured using an Olympus Vanox research microscope equipped with a 3-CCD Camera (Model Del-750) and analyzed with the "NIH-Image" v1.60 public domain program developed at the National Institutes of Health and available at <http://zippy.nimh.nih.gov/pub/nih-image>. The high quality of the sections used allowed for direct visualization and quantification of intermediate stages and also glomerulotubular structures of developing kidney throughout the entire length of the section.

Cell Cultures/ siRNA Transfection

The mK3 and mK4 cells were kindly provided by Stephen Potter (Children's Hospital Medical Center, Cincinnati, OH, USA). Cells were seeded in 12-well plates and cultured Dulbecco's modified Eagle's medium supplemented with 10%

fetal bovine serum. At approximately 50% confluence, siRNA duplexes were transfected into the cells with siPORT Lipid (Ambion, Austin, TX, USA). 6 μ L of a 20 μ mol/L stock solution of siRNA targets was transfected in each well to achieve a final concentration of 120 nmol/L. Total protein was harvested 36 to 48 h after transfection using M-PE Extraction Reagent (Pierce Biotechnology, Rockford, IL, USA). The double stranded RNA (siRNA) used to target *Ahr* was: Sense: 5'-GGGCCAAGAGCUUCUUUGAtt-3'; and Antisense: 5'-UCAAGAAGCUCUUGGCCc-3'. A silencing scrambled siRNA negative control (Ambion) was used in all experiments. In rescue experiments, mK4 cells were transfected with 2 μ g of CB6⁺-*Wt1* (-/-) plasmid encoding for 52 kDa *Wt1* protein or empty vector 24 h after transfection with siRNA. After 48 h, protein and RNA were harvested for further analysis.

Protein Harvesting

Metanephroi were washed with PBS and homogenized in T-PER Tissue Extraction Reagent (Pierce Biotechnology). Total protein or diffracted proteins (cytoplasmic and nuclear) were harvested using M-PER and NE-PER Extraction Reagents (Pierce Biotechnology), respectively, as described by the manufacturer. Protein concentration was measured by the method of Bradford. Cytoplasmic and nuclear fractions were separated using NE-PER (Pierce Biotechnology) as per manufacturer's instructions with the addition of HALT protease inhibitor (Pierce Biotechnology). Protein concentrations were determined by Bradford using albumin standards created with the CERI and NER reagents.

Western Analysis

Protein samples were boiled for 2 min and applied to 4% to 12% NuPAGE Bis-Tris gels (Invitrogen, Carlsbad, CA, USA). Twenty micrograms of protein were loaded onto a 4% to 12% Bis-Tris gel (Invitrogen) and run in MOPS buffer under reduced conditions.

Table 1. PCR primers.

Gene	Forward primer 5'-3'	Reverse primer 5'-3'	Size	Annealing temperature
18S	CGTCTGCCCTATCAACTTTCG	GCCTGCTGCCTTCCTTGG	130 bp	55°C
<i>Cyp1a1</i>	TCGTGTCAGTAGCCAATGTC	GCATCCAGGGAAGAGTAGG	178 bp	55°C
<i>E-cadherin</i>	CGACCCCTGCCTCTGAATCC	CTTTGTTCTTTGTCCCTGTGG	175 bp	55°C
<i>Epidermal growth factor receptor</i>	GAGGAGGAGAGGAGAACTG	GGTGGGCAGGTGTCTTTG	196 bp	55°C
<i>Insulin-like growth factor 1 receptor</i>	GTCCCTCAGGCTTCATCC	GAGCAGAAGTCACCGAATC	126 bp	55°C
<i>Insulin-like growth factor 2 receptor</i>	AGTATGTGAACGGCTCTG	TCTGTGATTGTCTGGATAGG	184 bp	55°C
<i>Lim homeobox protein 1</i>	ACCTAAGCAACAACACTACAATC	AACACGGGAGTAGAAAAGC	167 bp	55°C
<i>Paired box gene 2</i>	AGGTTTACATCTGGTCTGG	TAGGAAGGACGCTCAAAG	162 bp	55°C
<i>Retinoic acid receptor α</i>	CCCAGAAGACTAAAGTTGAC	TGGCAGGTAGTTGTGATG	152 bp	55°C
<i>Secreted frizzled-related sequence protein 1</i>	GCAGTTCTTCGGCTTCTA	ATGGAGGACACACGGTTG	134 bp	55°C
<i>Syndecan 1</i>	GAGAACAAGACTTCACCTTTG	GCACCTTCCTCCTGTCC	139 bp	55°C
<i>Taurine transporter</i>	CATCCATCGTCATTGTGTC	AAGTTGGCAGTGCTAAGG	196 bp	55°C
<i>Wingless-related MMTV-integration site 4</i>	GTAGCCTTCTCACAGTCCTTTG	GGTACAGCACGCCAGCAC	188 bp	55°C
<i>Wilms tumor suppressor 17aa</i>	CCTGAGGACGCCCTACAGC	CTGTGCCGTGGTTGCTCTGC	161 bp	55°C
<i>Wilms tumor suppressor +KTS</i>	AGCTCAAAAGACACCAAAGGAG	GAAGGGCTTTTCACTTGTTTAC	137 bp	55°C
<i>Wilms tumor suppressor -KTS</i>	AGCTCAAAAGACACCAAAGGAG	GGGCTTTTCACTGTATGAG	125 bp	55°C

After electrophoresis, proteins were transferred to PDVF membranes and probed with three different Wt1 antibodies (Wt1 N-[180]: sc-846, Santa Cruz Biotechnology, Santa Cruz, CA, USA]; C19 [Santa Cruz Biotechnology] and H2-F6 [Chemicon International, Temecula, CA, USA] or Ahr antibody [BioMOL Research Laboratories Inc., Plymouth Meeting, PA, USA]). Signals were visualized with horseradish peroxidase conjugated secondary antibody. Proteins were transferred to a PVDF membrane and probed for the nuclear transcription factor Oct1 (SC-232) or the cytoplasmic protein HSP90 α/β (SC-13119) (Santa Cruz Biotechnology). Signals were visualized with a corresponding secondary antibody and chemiluminescence detection using ECL+ (Amersham Biosciences, Little Chalfont, Buckinghamshire, UK).

Membranes were developed using the enhanced chemiluminescent (SuperSignal West Dura) Western blotting system (Pierce Biotechnology). Three to five independent experiments were performed in all instances.

RNA Isolation

Total RNA was extracted from the cells using TRI reagent (Molecular Research

Center Inc., Cincinnati, OH, USA) according to manufacturer's specifications.

RT-PCR

Reverse transcription was performed with MuLV Reverse transcriptase (Applied Biosystems, Foster City, CA, USA) and OligoDTs according to manufacturer's specifications. PCR was performed using DNA Taq Polymerase (Applied Biosystems) using specific primers and PCR thermoprofile sets for each gene. Primer sequences and PCR conditions for *Cyp1a1* and *E-cadherin* were as published by Reiners *et al.* (17) and Hosono *et al.* (18). Primers used to detect specific sequences in the 5' UTR region of *Wt1* upstream of both AUGs are listed in Table 1. Owing to the high G-C rich content of the *Wt1* 5' UTR region, PCR was performed using Advantage-GC 2 Polymerase (BD Biosciences, San Diego, CA, USA) according to manufacturer's specifications. PCR reaction was carried out at 94°C for 3 min, 68°C for 30 s, and 72°C for 3 min for 35 cycles and the reaction incubated at 72°C for 5 min.

Real-Time PCR Amplification

Reverse transcription of RNA was carried out using the iScript cDNA Synthesis Kit (BIO-RAD, Hercules, CA, USA). Real-

time PCR amplification was performed using the iCycler Detection System (BIO-RAD). For each run, 25 μ L of 2 \times SYBR Supermix (BIO-RAD) and 300 nmol/L for both forward and reverse primers in a total volume of 50 μ L were mixed. The thermal cycling conditions comprised an initial denaturation step at 95°C for 10 min, 50 cycles at 95°C for 15 s and 65°C for 1 min. All experiments were performed in triplicate. Primer sequences for mice *Wnt-4*, *Igf-1* rec. and *sfrp-1* are also listed in Table 1. 18S rRNA was used as an internal control for all measurements. Quantification was performed using comparative ($\Delta\Delta C_T$) method as described by Peinnequin *et al.* (19).

Statistical Analysis

Statistical significance was determined by analysis of variance (ANOVA) followed by LSD *post hoc* tests at the $P < 0.05$ level.

RESULTS

To examine the role of AHR during nephrogenesis *in vivo*, renal cell differentiation was monitored in GD:14 embryos of *Ahr*^{+/+} and *Ahr*^{-/-} mice. Renal blastema in the proliferation zone was less condensed in developing kidneys from *Ahr*^{-/-} embryos (Figure 1A). Morphomet-

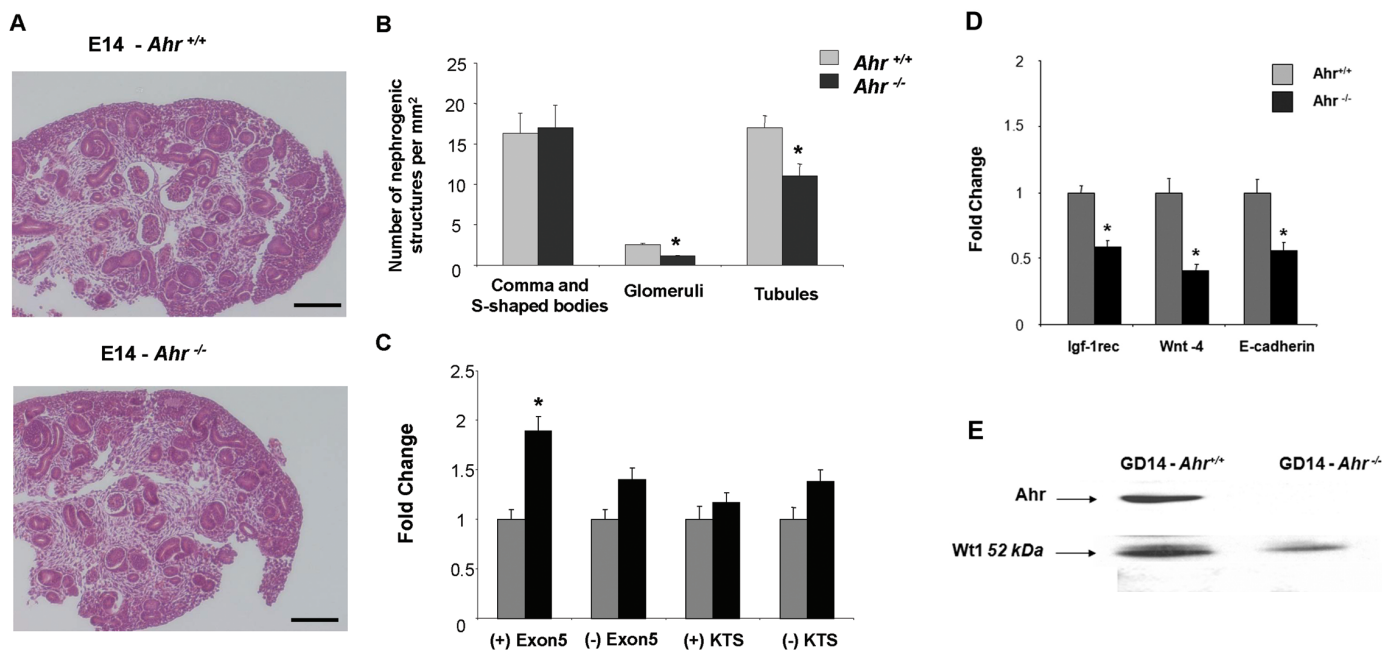


Figure 1. Deficits in renal differentiation and Wt1 expression in embryonic kidneys from *Ahr*^{-/-} mice. Kidneys were harvested from mouse embryos at GD:14 and fixed *in situ* for morphological examination as described. (A) Renal blastema in the proliferation zone was less condensed in developing kidneys from *Ahr* knockout embryos relative to wild-type counterparts (compare panels 1 and 2). Magnification in both panels was 289X. Similar findings were made in 10 mice from multiple litters. (B) Morphometric analyses of kidney sections showed decreased numbers of glomeruli and tubulo-epithelial structures ($P < 0.05$), despite equal numbers of comma and S-shaped bodies in *Ahr* knockout compared with wild-type mice. Data are presented as the average number of structures \pm SD for multiple sections. Measurements were taken from serial sections from 6 to 8 embryonic kidneys isolated from three or more dams. The values shown represent the composite of serial sections with variance expressed as the difference between values for each kidney per mouse strain. (C) PCR analyses of Wt1 splice variants in embryonic kidneys of *Ahr*^{-/-} compared with wild-type mice. (D) PCR analysis of various markers of renal cell differentiation (*Igf-1 rec*, *Wnt4* and *E-cadherin*) in embryonic kidneys from *Ahr*^{-/-} and *Ahr*^{+/+} mice. (E) Western blot analysis of Ahr and Wt1 in kidneys of *Ahr*^{-/-} and *Ahr*^{+/+} mice. One representative experiment out of two is shown. Equal protein loadings were confirmed based on the signal obtained with the same antibody for a nonspecific band (80 kDa).

ric analysis revealed decreased numbers of glomeruli and tubuloepithelial structures in *Ahr*^{-/-} mice after normalization by area, with equal numbers of comma and S-shaped bodies (Figure 1B). The embryonic kidneys of *Ahr*^{-/-} mice expressed higher levels of the (+) 17aa Wt1 splice variant (Figure 1C), a change that correlated with lower levels of *Igf-1 rec*, *Wnt-4* and *E-cadherin* mRNAs and reduced levels of 52 kDa Wt1 protein (Figures 1D, E). Immunological detection experiments established colocalization of the Wt1 and Ahr proteins in developing metanephric glomeruli, as well as in the adult glomeruli (Figures 2A–F).

A gene knockdown approach was employed to examine the role of AHR in genetic programming and MET in embryonic mK3 and mK4 cell lines, models of

early uninduced and later-induced murine metanephric mesenchyme, respectively (20). The mK3 cells exhibited spindle-shaped morphologies with irregular cytoplasmic projections, while mK4 cells exhibited cobblestone morphologies and polygonal shapes (Figure 3A). The degree of cellular differentiation in these lines was monitored based on the expression of genes involved in MET. mK4 cells expressed higher levels of *Igf-1 rec*, *Wnt-4* and *E-cadherin* mRNAs compared with mK3 cells, while transcript levels for *Bf-2* and secreted *sFrp-1* were higher in mK3 cells (Figure 3B). The pattern of Wt1 protein expression in these cell lines was striking, with the 52 kDa Wt1 protein isoform detected predominantly in mK4 cells; but higher levels of the two lower 40 kDa isoforms corresponding to the (\pm)

exon 5 variants predominantly the (+) 17 AA 40 kDa were noted in mK3 cells (Figure 3C). The specificity of the Wt1 40 kDa signal in Western blot experiments was verified using a H2-F6 Wt1 antibody that selectively recognizes the larger 52 and 62 kDa isoforms of Wt1 protein. The mK4 cells expressed higher cytoplasmic and nuclear levels of Ahr protein than mK3 cells (see Figure 3C), suggesting that expression of both Ahr and Wt1 proteins correlates with the degree of renal cell differentiation. The purity of fractions was confirmed using HSP90 α/β and Oct1 as markers of cytoplasmic and nuclear identity, respectively (Figure 3D).

Ahr protein levels decreased by 50% to 70% in mK4 cells transfected with *Ahr* siRNA, and remained unchanged in cells treated with scrambled RNA (Figure 4A).

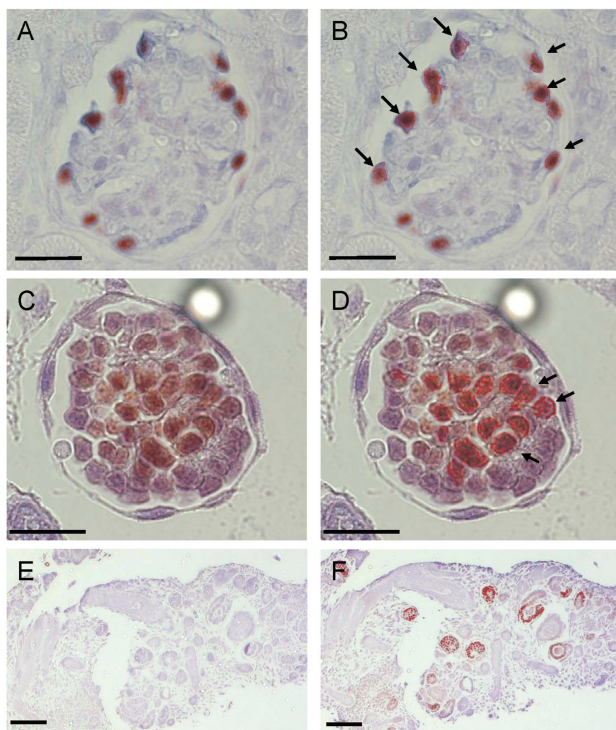


Figure 2. Ahr and Wt1 colocalize in the developing and adult kidney. Dual immunohistochemical analyses of Ahr and Wt1 proteins visualized using 3, 3', 5, 5'-tetramethylbenzidine (TMB) and NovaRED, respectively (Vector Laboratories Burlingame, CA, USA). Panels A and C are representative images taken of glomeruli from adult C57BL/6J mouse kidneys or GD 11 cultured metanephros cross sections. In panel B, maximal Ahr signal (blue color) was set to threshold in serial sections processed for Ahr alone using Zeiss Axiovision Rel 4.3 image analysis. The thresholded filter was applied to dual-stained sections resulting in a red-outlined area of positive maximal Ahr signal. Ahr-Wt1 colocalization was defined by a positive nuclear Wt1 signal in proximity to the outlined maximal Ahr signal, as denoted by arrows. Because of the diffuse Ahr signal throughout metanephric glomerular cells, in panel D, Ahr-Wt1 colocalization was determined by thresholding for color resulting from both Ahr and Wt1 signals and compared with control serial sections stained for each antibody alone. The analysis showed Ahr-Wt1 colocalization outlined in red and only 10% errant signal detected in control sections. Panels E and F are serial cross sections of C57BL/6J GD 11 cultured metanephros analyzed for Ahr alone or Ahr-WT1 colocalization as described above. In panels A-D the scale represents 25 μm , while in panels E and F the scale represents 100 μm .

The efficiency of the *Ahr* knockdown was examined in mK4 cells treated for 16 h with benzo(a)pyrene, a hydrocarbon ligand of Ahr that activates *Cyp1a1* via transcriptional mechanisms (21). *Cyp1a1* mRNA levels increased two-fold in benzo(a)pyrene-treated cells, and knockdown of Ahr protein abolished this effect (Figure 4B, C). The influence of AHR on *Wt1* mRNA was examined next by RT-PCR using a primer set that hybridizes to the 5' UTR region upstream of both the

52 and 40 kDa isoform translation start sites, and that recognizes all major *Wt1* variants. No alterations in total mRNA levels were observed following *Ahr* knockdown (Figure 5A). Next, the expression of *Wt1* splice variants generated by both exon 5 and 9 splicing was examined by real time PCR. Four different set of primers were used to specifically recognize each of the splice variants including, (+) 17AA, (-) 17AA, (+) KTS, and (-) KTS. We conclude that the primer set

used to amplify (+) 17AA only recognizes this splice variant and discriminates between (+) and (-) 17AA variants. Ahr knockdown caused a pronounced increase in the (+) 17aa splice variant in mK4 cells (Figure 5B), while other *Wt1* splice variants did not change. A reduction of cellular Ahr protein levels caused a significant reduction in 52 kDa *Wt1* protein levels, while the levels of (+) 17aa 40 kDa isoform increased which is consistent with the increases in the mRNA level for this *Wt1* splice variant (Figure 5C). These findings were consistent with morphological shifts of mK4 cells toward the lesser differentiated mK3 phenotype (not shown). Together, these data implicate Ahr in posttranscriptional regulation of *Wt1* in embryonic kidney cells.

To determine if posttranscriptional deregulation of *Wt1* by AHR is of functional consequence during the course of renal cell differentiation, the expression of downstream effector genes in nephrogenesis was examined by RT-PCR. Marked decreases in *Igfr-1 rec.*, *Wnt-4* and *sFrp-1* were observed following Ahr knockdown in mK4 cells (Figure 6). To confirm the role of WT1 in the regulation of the downstream targets, siRNA degradation of WT1 was examined. siRNA-induced degradation of *Wt1* downregulated markers of epithelial identity (*Igf-1 rec.*, *Igf-2 rec.*, *Wnt-4* and E-cadherin), and either enhanced markers of mesenchymal identity such as *sfrp1* (Figure 7A). No changes in *Lhx1*, a marker of renal vesicle and nephron progenitors, were observed with this treatment. Importantly, *Wt1* silencing downregulated direct targets of *Wt1* transcriptional control, confirming the usefulness of these markers to examine the differentiation state of developing kidneys (Figure 7B). To determine if these genes are regulated as a direct result of AHR-mediated interference with *Wt1*, mK4 cells were transfected for 24 h with CB6-*Wt1*, a plasmid encoding (-) 17aa / (-) KTS 52 kDa *Wt1* protein, or empty vector, after downregulation of Ahr. Reduced *Wt1* protein levels following *Ahr* knockdown were restored in mK4 cells transfected with *Wt1* cDNA compared

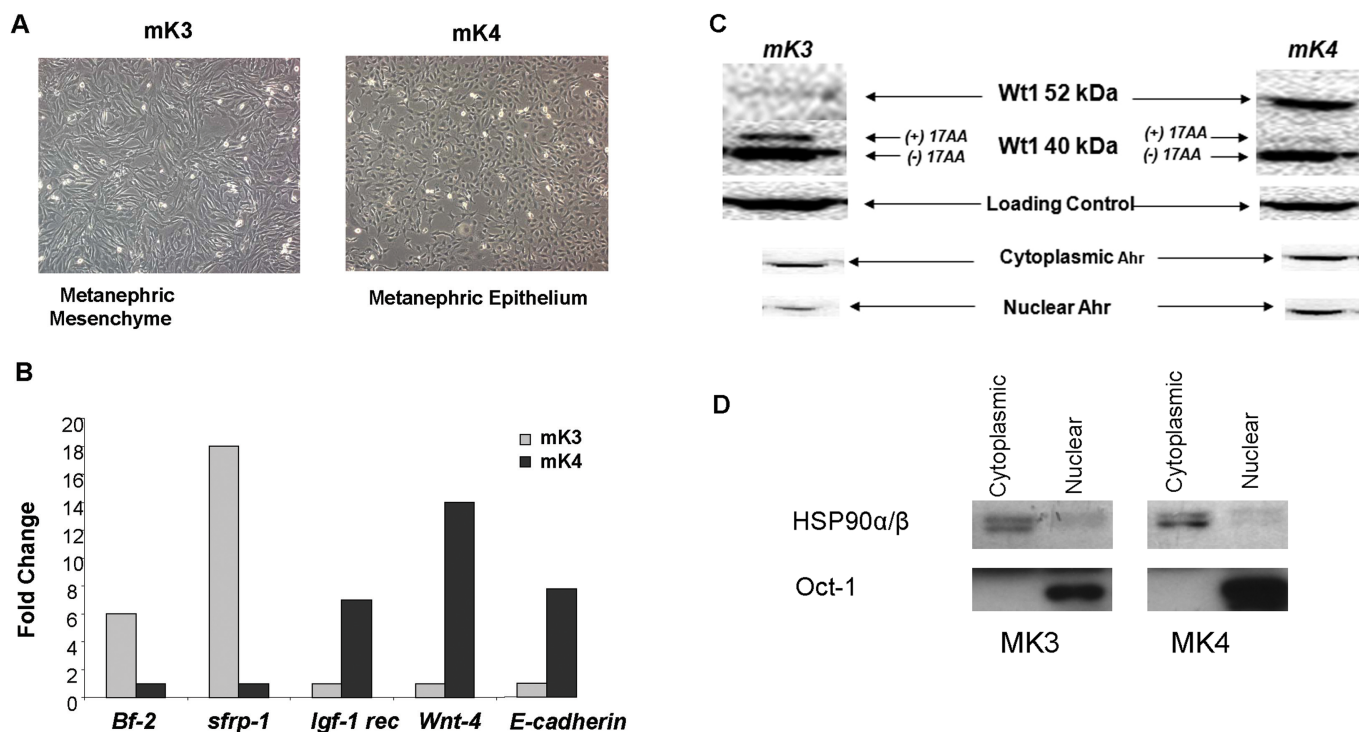


Figure 3. Differentiation and epithelialization status in mK3 and mK4 embryonic kidney cell lines. The expression of renal cell differentiation and epithelialization marker genes was examined by PCR or Western blot analysis. (A) The mK3 cells exhibited a spindle-shape morphology with irregular cytoplasmic projections, while mK4 cells displayed polygonal shapes indicative of later stage differentiation during the course of MET. (B) Real time or RT-PCR analyses showed that mK4 cells expressed higher level of *E-cadherin*, *Wnt-4* and *Igf-1 rec* compared with mK3 cells. In contrast *Bf-2* and secreted *frizzled receptor binding protein-1 (sfrp-1)* transcripts were higher in mK3 cells. Similar results were seen in three different experiments. (C) Western blot analysis showed that mK4 cells possess higher levels of Ahr and 52 kDa Wt1 protein compared with mK3 cells. Similar results were seen in four separate experiments. (D) The quality of cellular fractions was confirmed by Western blotting using HSP90α/β and Oct1 as markers of cytoplasmic and nuclear proteins, respectively. Images shown are representative of triplicate samples from multiple gels. Equal protein loadings were confirmed based on the signal obtained with the same antibody for a nonspecific band (80 kDa). Notably, embryonic kidney cell lines also expressed 40 kDa variants of ± exon 5. The abundance of (+) 17 AA variant inversely correlated with the degree of renal cell differentiation as shown by decreases in *Bf-2* and *sfrp-1* mRNAs and increases in *Igf-1 rec*, *Wnt-4* and *E-cadherin* mRNAs.

with empty vector, as determined by Western blot analysis (Figure 7C). Importantly, decreased *Igf-1 rec* and *Wnt-4* mRNA levels following Ahr knockdown were restored by the Wt1 cDNA, indicating that deregulation of these targets lies downstream of Ahr and is mediated by posttranscriptional deregulation of Wt1. Wt1 did not restore *sfrp-1* mRNA levels, indicating that regulation of this target is not directly mediated by *Ahr:Wt1* interactions, at least under the experimental conditions examined (Figure 7D).

DISCUSSION

A developmentally-regulated pattern of Ahr expression in the kidney was first

reported by Abbott *et al.* (22) who demonstrated that levels of Ahr protein are significantly higher in renal epithelial cells compared with mesenchymal cells, and downregulated by Ahr ligands. Bryant *et al.* (23) later showed that *Ahr* mRNA increases in metanephric tubules from GD:12–14, with continued expression throughout the life of the mouse. A casual link between Ahr and nephrogenesis was established in experiments showing that renal development is delayed in metanephric organ cultures of embryonic kidneys from *Ahr*^{-/-} mice, or following ligand-induced downregulation of Ahr protein (5). Here we show that Ahr is involved in the regulation of

developmentally-specific patterns of gene expression during MET in the kidney. Specifically, evidence is presented that: a) *Ahr*^{-/-} embryos exhibit delayed epithelialization compared with wild-type counterparts; b) AHR and WT1 protein levels correlate with the degree of cellular differentiation in mK3 and mK4 cell lines; c) downregulation of Ahr protein disrupts gene expression profiles and differentiation programs in embryonic kidney cells lines.

The essential role of Wt1 in kidney development was unequivocally established in studies showing that homozygous Wt1 knockout mice fail to develop metanephric kidneys and die *in utero* (7).

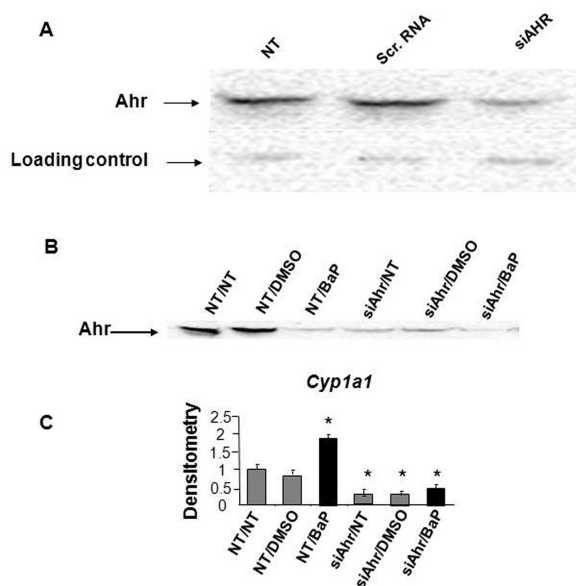


Figure 4. Downregulation of Ahr by siRNA in the mK4 embryonic kidney cell line. (A) Ahr protein levels decreased in mK4 cells transfected with siRNA directed at the AhR, while protein levels remain unchanged in cells treated with scrambled (scr) RNA as a nonspecific negative siRNA control. NT = no treatment. One representative experiment from a total of ten is shown. Equal protein loadings were confirmed based on the signal obtained with the same antibody for a nonspecific band (25 kDa). (B) Hydrocarbon inducibility of *Cyp1a1* is abolished in mK4 cells following Ahr siRNA transfection. (C) RT-PCR for *Cyp1a1* shows that only siRNA against Ahr inhibits *Cyp1a1* inducibility by BaP. One representative experiment out of three is shown. Densitometry is shown in arbitrary units. * denotes statistical differences from respective NT controls.

In homozygous *Wt1* knockout mice, the ureteric bud fails to grow out of the mesonephric duct and metanephric mesenchyme dies. *Wt1* is expressed selectively in metanephric blastema, S-shaped bodies and glomerular epithelium during kidney development, and confined to the podocyte layer of the mature nephrons (24). *Wt1* is mutated in a proportion of nephroblastomas, embryonic kidney tumors characterized histologically by incomplete epithelialization of the condensing renal mesenchyme. The evidence presented here indicates that Ahr plays a regulatory role during nephrogenesis and that this function is linked to regulation of the *Wt1* signaling. The observed reduction in numbers of glomeruli in Ahr null mice may be explained by developmental delay and/or direct interference with metanephric epithelialization in Ahr null mice. It is interesting to note that although the molecular and cellular pheno-

types elicited by BaP in the developing kidney are largely mediated by proteasome-mediated downregulation of AHR (25), BaP arrested metanephric differentiation at an earlier point than AHR null mice. These settled differences likely reflect the complexity of the biological response since disruption of metanephric differentiation by the carcinogen is known to involve AHR-dependent reactivation of repetitive sequences within the embryonic kidney genome (26,27).

Recent studies in this laboratory have shown that a coisogenic mouse strain expressing a functionally inactive D2N Ahr^d allele exhibits a 0.5- to 1-d delay in nephrogenesis compared with wild-type mice (25). Of note is that subtle renal deficits in renal cell differentiation associated with genetic loss of Ahr do not involve gross deficits in renal function, and only translate into reduced renal reserve capacity in Ahr null mice. Given that

Ahr^{-/-} embryos are viable at term, and do not exhibit overt deficits of renal structure, the pathogenetic consequences of delayed nephrogenesis seen in the absence of Ahr protein are likely coupled to deficits in renal function as mice continue to develop. Of note are reports showing that *Ahr*^{-/-} mice exhibit cardiac hyperplasia and hypertrophy (28); pathobiological processes involving altered *Wt1* functions.

RNA interference provided a complementary approach to gene ablation *in vivo* for the study of regulatory interactions between Ahr and *Wt1* during the course of nephrogenesis. These experiments helped to differentiate renal developmental deficits that are associated directly with loss of Ahr protein from changes that are secondary to long-term adaptation. The efficiency of the siRNA knockdown approach was confirmed by the loss of *Cyp1a1* inducibility in response to AHR activation by a hydrocarbon ligand in siRNA-treated cells. The downregulation of *Ahr* by siRNA altered the expression of (+) 17aa isoform in mK4 cells, suggesting that regulation of *Wt1* by Ahr is mediated at the posttranscriptional level. This interpretation is in keeping with the finding that interference with Ahr signaling was without effect on total *Wt1* mRNA levels. It should be noted that reciprocal interactions between *Wt1* and Ahr may not be directly linked to phenotypic outcomes, and instead, impact nephrogenesis indirectly through the regulation of differentiation status. Interestingly, *Ahr* knockdown in mK3 cells, a line that exhibits a lesser degree of metanephric differentiation, did not affect the ratio of (±) exon 5 splice variants, and instead caused a shift in KTS splice variants toward the (-) KTS phenotype (not shown). This finding is consistent with previous observations that downregulation of Ahr protein following extended hydrocarbon ligand treatment in metanephric cultures shifted the (±) KTS ratio toward the (-) KTS phenotype in an Ahr-dependent manner (5).

The loss of Ahr protein *in vivo* correlated with decreased levels of 52 kDa *Wt1* protein. Furthermore, expression of the

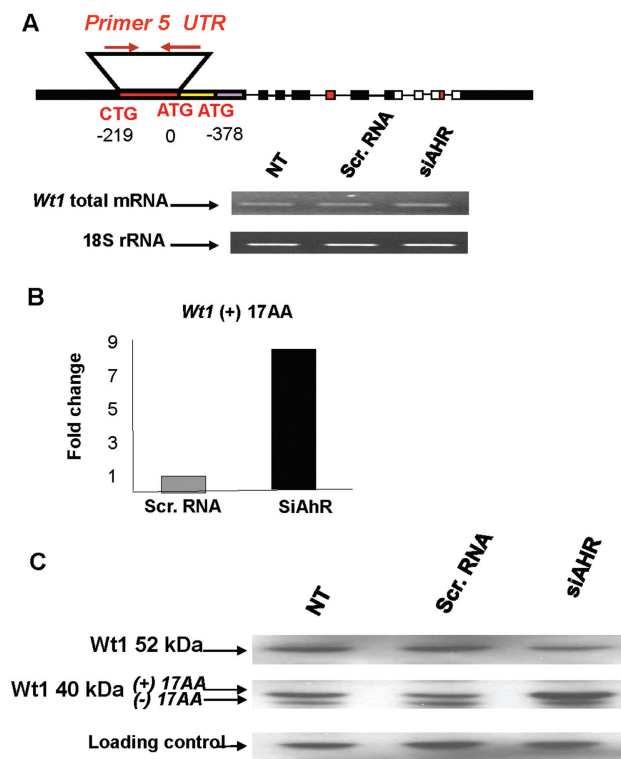


Figure 5. Regulation of Wt1 by Ahr. Expression profiles of Wt1 mRNA or protein were examined in mK4 cells following siRNA Ahr knockdown. (A) RT-PCR was performed using a primer set that hybridizes to the *Wt1* 5' UTR region upstream of the translation start sites for the 52 and 40 kDa isoforms. Ahr knockdown did not alter total Wt1 mRNA levels. The signal for 18S rRNA is shown as a normalization control. (B) Real time PCR was performed using primer sets specific for the (±) KTS and (±) 17 AA Wt1 splice variants. Scr = scrambled. Ahr knockdown caused a pronounced increase in (+) 17 AA Wt1 expressions in mK4 cells. (C) Western blot analysis showed that Ahr knockdown caused selective decreases in 52 kDa Wt1 protein isoform and corresponding increases in 40 kDa isoforms. A nonspecific ~80-kDa protein recognized by the Wt1 antibody was used as a loading control. Similar results were seen in four different experiments.

40 kDa Wt1 isoforms was correlated inversely with the degree of renal cell differentiation. A mechanistic link between Wt1 isoforms and Ahr is consistent with the finding that downregulation of Ahr protein in mK4 cells shifted the pattern of Wt1 expression from the mature 52 kDa isoform to the lower molecular weight isoforms. These findings suggest that these Wt1 isoforms support different cellular functions, an interpretation that is consistent with shifts in Wt1 protein expression profiles in mK3 cells compared with mK4 cells. Whether regulation of Wt1 splicing is a result of direct interactions of Ahr with the cellular splicing machinery, or involves exon skipping, or

changes in mRNA stability is not known.

The relevance of functional Ahr/Wt1 interactions was monitored based on the expression of *Bf-2*, *srrp-1*, *Igf-1rec.* and *Wnt-4*. These genes play essential roles during MET in nephrogenesis, with *Igf-1rec.*, *Wnt-4* and *E-cadherin* recognized as downstream targets of Wt1 during the course of renal cell differentiation and nephrogenesis (29,30). A role for *Igf-1rec.* in renal cell differentiation is well documented, with ubiquitous expression found to be developmentally regulated during metanephric maturation, and enhanced during tubulogenesis (31). *Wnt-4* is a mesenchymal signal for epithelial transformation of metanephric mes-

enchyme in the developing kidney, and is expressed in pre-tubular mesenchymal cells shortly before aggregation and transformation into epithelial tubules (32). *Wnt* signaling is initiated by interaction of the Wnt protein with frizzled receptors (33). In addition to the membrane-bound forms of frizzled, several genes encoding soluble homologous proteins have been identified (34). These secreted frizzled-related proteins bind Wnt in the developing metanephros and function as modulators of Wnt signaling. *E-cadherin* is recognized as a Wt1 target gene (18), and a regulator of the epithelial phenotype. In keeping with their unique functions during the course of renal cell differentiation, mK4 cells were found to express higher levels of *Igf-1 rec.*, *Wnt-4* and *E-cadherin* than the lesser differentiated mK3 cells. In contrast, the expression of *Bf-2* and *sFrp-1* was higher in mK3 than mK4 cells. Both AHR and WT1 increased as a function of renal cell differentiation status *in vitro* and *in vivo*, suggesting that these proteins are functionally linked in the regulation of MET.

AHR functions as a transregulator of gene expression during the course of mammalian cell differentiation (35). A role for AHR in posttranscriptional control of gene expression has not been recognized previously. Thus, the influence of AHR on developmentally-regulated expression of *Wt1* splice variants during renal differentiation is intriguing. The relevance of these findings is emphasized by reports that differential splicing of exon 5 occurs in human kidneys and in Wilms tumor samples (9). While the ±KTS sequence is conserved throughout the species, and necessary for renal development, exon 5 is only present in placental mammals and is not required for nephrogenesis, implantation or lactation (36). Evidence for participation of exon 5 in transcriptional repression or Par4 binding suggests a possible role of this variant in the regulation of Wt1 expression in differentiated cells such as podocytes (37,15). Thus, future studies should investigate the role of AHR and exon 5 variants of Wt1 in the regulation of renal cell differentiation. The

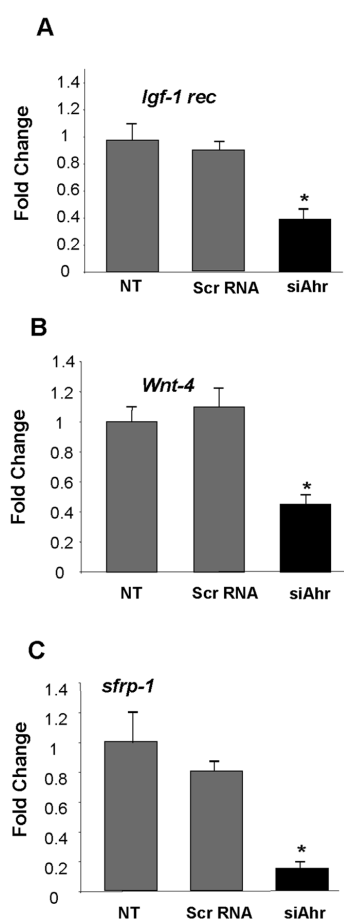


Figure 6. Ahr plays a regulatory role in programming of MET and differentiation of mK4 cells. Real time PCR was performed using specific primers for various molecular targets to determine the expression of effector genes essential in nephrogenesis. Ahr knockdown in mK4 caused a significant decreases in mRNA levels for *Igf-1 rec*. (A), *Wnt-4* (B), and *sfrp-1* (C) (* $P < 0.05$). One representative experiment out of three is shown. NT = no treatment; Scr = scrambled.

involvement of AHR in the regulation of murine nephrogenesis raises important questions about its role in human kidney development and the linkage between prenatal exposures to AHR ligands and deficits in renal developmental programming (13,14,22,23,38).

ACKNOWLEDGMENTS

This study was supported by NIH Grants ES04917, ES012542 and ES014443.

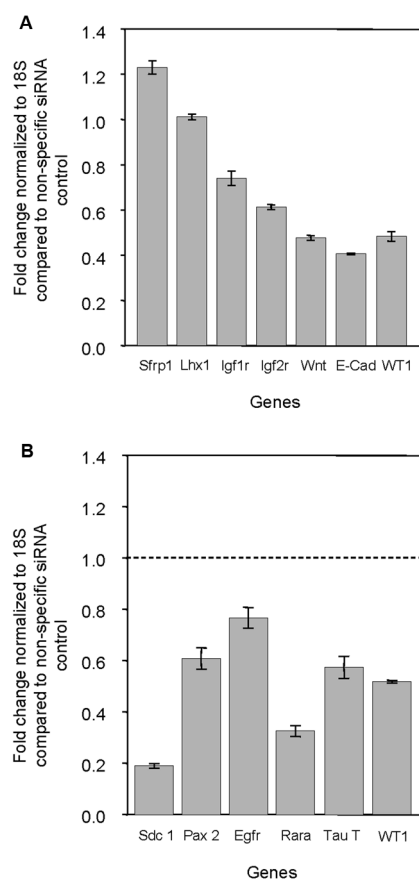
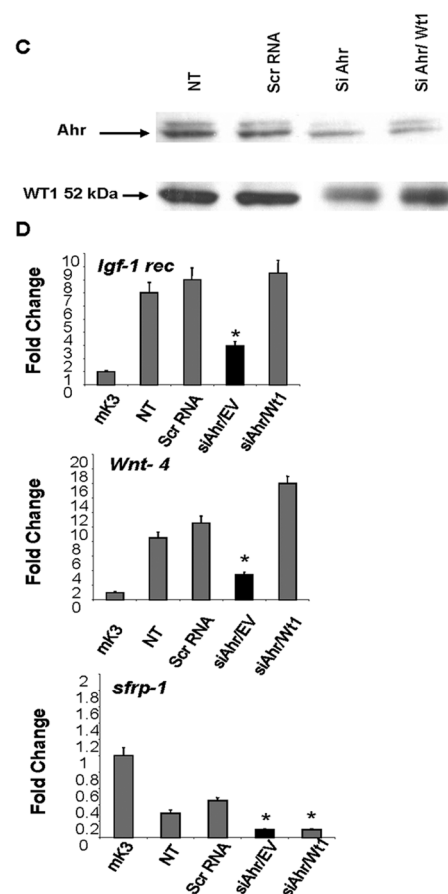


Figure 7. Interactions between Ahr and Wt1 during the course of renal cell differentiation. (A) Downregulation of markers of differentiation by Wt1 siRNA. mK4 cells were cultured in the presence of Wt1 siRNA for 3 d. qRT-PCR values were calculated to represent fold change normalized to 18S compared with nonspecific siRNA control. *sfrp-1* and *lim 1* homeobox gene were used as markers of mesenchymal identity, while *Igf-1 rec*, *Igf-2 rec*, *Wnt4*, and *E-cadherin* were used as markers of epithelial identity. (B) Deregulation of Wt1 targets by Wt1 siRNA. mK4 cells were cultured in the presence of Wt1 siRNA for 3 d. qRT-PCR values were calculated to represent fold change normalized to 18S compared with nonspecific siRNA control. *Syndecan1*, *paired box protein 2*, *EGF rec*, *retinoic acid receptor alpha*, *taurine transporter*, and *Wilms tumor transcription factor*. (C) The mK4 cells were transfected for 24 h with the CB6-Wt1 (-) exon 5/ (-) exon 9 plasmid encoding for 52 kDa Wt1 protein or empty vector after transfection with Ahr siRNA. Reduced Wt1 protein levels following Ahr knockdown were rescued in cells transfected with Wt1 cDNA compared with empty vector. (D) Real time PCR shows decreased mRNA levels for *Igf-1 rec* and *Wnt-4* following Ahr knockdown and effective rescue in cells transfected with Wt1 cDNA; however, decreases in *sfrp-1* mRNA following Ahr knockdown were not restored in cells transfected with Wt1 cDNA. One representative experiment out of three is shown. NT = no treatment.

The authors wish to thank Steven Potter (Children's Hospital Medical Center, Cincinnati, OH, USA) for providing the mK3 and mK4 cell lines, Aart G Jochemsen (Leiden University Medical Center, Leiden, The Netherlands) for Wt1 cDNA plasmids and Vilius Stribinskis for help-



ful discussions. The assistance of Marlene Steffen and Diego Montoya is gratefully acknowledged.

DISCLOSURE

The authors declare that they have no competing interests as defined by *Molecu-*

lar Medicine, or other interests that might be perceived to influence the results and discussion reported in this paper.

REFERENCES

- Barker DJ, Winter PD, Osmond C, Margetts B, Simmonds SJ. (1989) Weight in infancy and death from ischaemic heart disease. *Lancet*. 2:577–80.
- Lim K, Armitage JA, Stefanidis A., Oldfield BJ, Black MJ. (2011). Intrauterine growth restriction in the absence of postnatal ‘catch-up’ growth leads to improved whole body insulin sensitivity in rat offspring. *Pediatr. Res.* [Epub ahead of print].
- Menendez-Castro C, et al. (2011), Early and late postnatal myocardial and vascular changes in a protein restriction rat model of intrauterine growth restriction. *PLoS One*. 6:e20369.
- Nanez A, Ramos KS. (2010) Introduction and Overview of Receptor Systems. In: *Comprehensive Toxicology*. 2nd ed. Vol. 2. McQueen CA (editor in chief). Elsevier, San Diego, pp. 71–80. Available at: http://www.knovel.com/web/portal/browse/display?_EXT_KNOVEL_DISPLAY_bookid=3459&VerticalID=0
- Falahatpisheh MH, Ramos KS. (2003) Ligand-activated Ahr signaling leads to disruption of nephrogenesis and altered Wilms’ tumor suppressor mRNA splicing. *Oncogene*. 22:2160–71.
- Bittinger MA, Nguyen LP, Bradfield CA. (2003) Aspartate aminotransferase generates proaggonists of the aryl hydrocarbon receptor. *Mol. Pharmacol.* 64:550–6.
- Kreidberg JA, et al. (1993) WT-1 is required for early kidney development. *Cell*. 74:679–91.
- Menke AL, van der Eb AJ, Jochemsen AG. (1998) The Wilms’ tumor 1 gene: oncogene or tumor suppressor gene? *Int. Rev. Cytol.* 181:151–212.
- Iben S, Royer-Pokora B. (1999) Analysis of native WT1 protein from frozen human kidney and Wilms’ tumors. *Oncogene*. 18:2533–6.
- Wang ZY, Qiu QQ, Gurrieri M, Huang J, Deuel TF (1995). Wt1, the Wilms’ tumor suppressor gene product, represses transcription through an interactive nuclear protein. *Oncogene*. 10:1243–7.
- Englert C, et al. (1995). Truncated wt1 mutants alter the subnuclear localization of the wild-type protein. *PNAS*. 92:11960–4.
- Wagner KD, Wagner N, Schedl A. (2003) The complex life of WT1. *J. Cell Sci.* 116:1653–8.
- Hammes A, et al. (2001) Two splice variants of the Wilms’ tumor 1 gene have distinct functions during sex determination and nephron formation. *Cell*. 106:319–29.
- Barboux S, et al. (1997). Donor splice-site mutations in WT1 are responsible for Frasier syndrome. *Nat. Genet.* 17:467–70.
- Richard DJ, Schumacher V, Royer-Pokora B, Roberts SGE. (2001) Par4 is a coactivator for a splice isoform-specific transcriptional activation domain in WT1. *Genes. Dev.* 15:328–39.
- Renshaw J, King-Underwood L, Pritchard-Jones K. (1997) Differential splicing of exon 5 of the Wilms tumour (WT1) gene. *Genes Chromosomes Cancer*. 19:256–66.
- Reiners Jr JJ, Jones CL, Hong N, Myrand SP. (1998) Differential induction of Cyp1a1, Cyp1b1, Ahd4, and Nmo1 in murine skin tumors and adjacent normal epidermis by ligands of the aryl hydrocarbon receptor. *Mol. Carcinog.* 21:135–46.
- Hosono S, et al. (2000) E-cadherin is a WT1 target gene. *J. Biol. Chem.* 275:10943–53.
- Peinnequin A, et al. (2004) Rat pro-inflammatory cytokine and cytokine related mRNA quantification by real-time polymerase chain reaction using SYBR green. *BMC Immunol.* 5:3.
- Valerius MT, Patterson LT, Witte DP, Potter SS. (2002) Microarray analysis of novel cell lines representing two stages of metanephric mesenchyme differentiation. *Mech. Dev.* 112:219–32.
- Whitlock Jr JP. (1999) Induction of cytochrome P4501A1. *Annu. Rev. Pharmacol. Toxicol.* 39:103–25.
- Abbott BD, Perdew GH, Buckalew AR, Birnbaum LS. (1994) Interactive regulation of Ah and glucocorticoid receptors in the synergistic induction of cleft palate by 2,3,7,8-tetrachlorodibenzo-p-dioxin and hydrocortisone. *Toxicol. Appl. Pharmacol.* 128:138.
- Bryant PL, Clark GC, Probst MR, Abbott BD. (1997) Effects of TCDD on Ah receptor, ARNT, EGF, and TGF-alpha expression in embryonic mouse urinary tract. *Teratology* 55:326–37.
- Pritchard-Jones K, et al. (1990) The candidate Wilms’ tumour gene is involved in genitourinary development. *Nature*. 346:194–7.
- Nanez A, Ramos IN, Ramos KS. (2011) A mutant AHR allele protects the embryonic kidney from hydrocarbon-induced deficits in fetal programming. *Environ. Health Perspect.* 2011 Jul 29 [Epub ahead of print].
- Teneng I, Stribinskis V, Ramos KS. (2007) Context specific regulation of LINE-1. *Genes Cells*. 12:1101–10.
- Ramos KS, Montoya-Durango DE, Teneng I, Nanez A, Stribinskis V. (2011) Epigenetic control of embryonic renal cell differentiation by L1 retrotransposon. *Birth Defects Res. A. Clin. Mol. Teratol.* 91:693–702.
- Thackaberry EA, et al. (2003) Insulin regulation in AhR-null mice: embryonic cardiac enlargement, neonatal macrosomia, and altered insulin regulation and response in pregnant and aging AhR-null females. *Toxicol. Sci.* 76:407–17.
- Sim EUH, et al. (2002) Wnt-4 regulation by the Wilms’ tumor suppressor gene, WT1. *Oncogene*. 21:2948–60.
- Werner H, Roberts Jr CT, Rauscher 3rd FJ, LeRoith D. (1996) Regulation of insulin-like growth factor I receptor gene expression by the Wilms’ tumor suppressor WT1. *J. Mol. Neurosci.* 7:111–23.
- Duong Van Huyen JP, et al. (2003) Spatiotemporal distribution of insulin-like growth factor receptors during nephrogenesis in fetuses from normal and diabetic rats. *Cell Tissue Res.* 314:367–79.
- Stark K, Vainio S, Vassileva G, McMahon AP. (1994) Epithelial transformation of metanephric mesenchyme in the developing kidney regulated by Wnt-4. *Nature*. 372:679.
- Vincan E. (2004) Frizzled/WNT signalling: the insidious promoter of tumour growth and progression. *Front. Biosci.* 9:1023–34.
- Yoshino K, et al. (2001) Secreted Frizzled-related proteins can regulate metanephric development. *Mech. Dev.* 102:45.
- Cheshire DR, Dunn TA, Ewing CM, Luo J, Isaacs WB. (2004) Identification of Aryl Hydrocarbon Receptor as a putative Wnt/β-Catenin pathway target gene in prostate cancer cells. *Cancer Res.* 64:2523–33.
- Natoli TA, et al. (2002) A mutant form of the Wilms’ tumor suppressor gene WT1 observed in Denys-Drash Syndrome interferes with glomerular capillary development. *J. Am. Soc. Nephrol.* 13:2058–67.
- Hewitt SM, Saunders GF. (1996) Differentially spliced exon 5 of the Wilms’ tumor gene WT1 modifies gene function. *Anticancer Res.* 16:621–6.
- Reiner J, Jones Jr C, Hong N, Myrand S. (1994) Differential induction of cyp1A1, cyp1B1, ahd4, and nmo1 in murine skin tumors and adjacent normal epidermis by ligands of the aryl hydrocarbon receptor. *Mol. Carcinog.* 21:135–46.